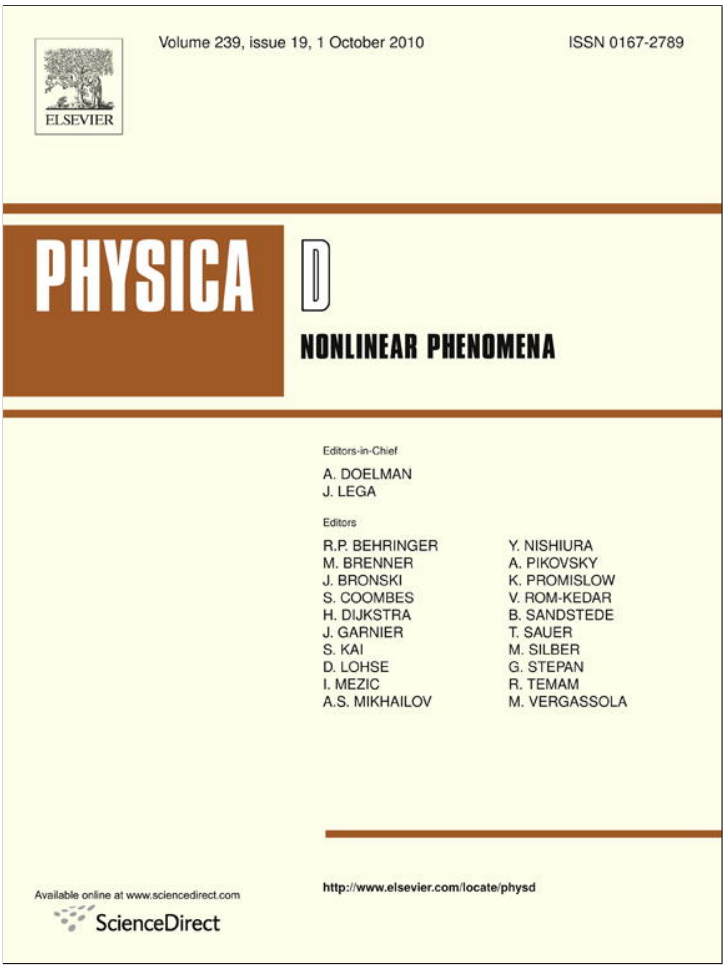

Physica D 239 (2010) 1855–1866

Contents lists available at ScienceDirect

Physica D

journal homepage: www.elsevier.com/locate/physd

A sharp-interface interpretation of a continuous density model for homogenization of gravity-driven flow in porous media

Daniel M. Anderson [a,*], Richard M. McLaughlin [b], Cass T. Miller [c]

[a] Department of Mathematical Sciences, George Mason University, Fairfax, VA 22030, United States

[b] Department of Mathematics, University of North Carolina, Chapel Hill, NC, 27599, United States

[c] Department of Environmental Sciences and Engineering, University of North Carolina, Chapel Hill, NC, 27599, United States

ARTICLE INFO

Article history:
Received 15 December 2008
Received in revised form
28 May 2010
Accepted 21 June 2010
Available online 28 June 2010
Communicated by H.A. Dijkstra

Keywords:
Homogenization
Sharp interface
Diffuse interface

ABSTRACT

We examine homogenization methods applied to sharp-interface and diffuse-interface models for gravity-driven flow in heterogeneous porous media. Our work specifically examines a matrix of models that includes (1) a variable media, diffuse-interface model, (2) a variable media, sharp-interface model, (3) a homogenized media, diffuse-interface model and (4) a homogenized media, sharp-interface model. We connect all four of these models via homogenization theory and sharp-interface limits. We show that existing results based on homogenization methods applied to sharp-interface models can be recovered by a less direct but more rigorous approach involving well-established homogenization theory and sharp-interface limits.

1. Introduction

Recent work by Miller and coworkers [1–3] has explored techniques for containing and/or mobilizing dense non-aqueous phase liquids (DNAPLs) in contaminated subsurface systems through the introduction of brine solutions. The success of such techniques relies on the accurate prediction of the location of the brine during the remediation stages as well as eventual brine recovery. The sequestration of carbon dioxide (CO_2) in deep geological reservoirs in order to combat large scale emissions of CO_2 into the atmosphere is another application in which the understanding of gravity-driven flows in complex porous media is of central importance. Here, for example, recent work has been directed towards the development of modeling and analysis tools that allow the prediction of time scales associated with the spread of subsurface CO_2 plumes and the reservoir storage efficiency (e.g. [4–6]).

For applications involving contaminated soil and other complex subsurface systems, in general it is necessary to examine and develop models that address heterogeneous media. Homogenization theory can be used in such contexts to extract from the full models, reduced models that, in an average sense, still account for the heterogeneities. The development of homogenization techniques that can be applied to situations that involve moving free boundaries, such as those occurring during remediation of contaminated soils using brine solutions and during the geological sequestration of CO_2, is therefore of considerable importance.

One important classification of models for free boundary problems relates to how one mathematically characterizes a boundary between two phases. Sharp-interface models introduce a mathematical dividing surface, whose thickness is zero, that separates one phase from another. Governing equations, such as conservation of mass and conservation of linear momentum, are given for each phase and conditions at the interface couple quantities in the bulk phases to dynamics of the interface. Diffuse-interface models, on the other hand, have an interfacial region that is defined implicitly in terms of level sets of field variables. For example, in a miscible system such as water and brine the species mass fraction varies continuously from some value in the bulk brine region to another value in the bulk water region. A diffuse interfacial region can be defined implicitly as the region between two level sets of species mass fraction. The actual thickness of such an interfacial region will depend on the specific choice of level sets, however, the physics of diffusion between the two phases sets the length scale in general. In the diffuse-interface model, a single set of governing equations applies over the whole domain, including the interfacial region.

* Corresponding author.
E-mail addresses: danders1@gmu.edu (D.M. Anderson), rmm@amath.unc.edu (R.M. McLaughlin), casey_miller@unc.edu (C.T. Miller).

0167-2789/$ – see front matter © 2010 Elsevier B.V. All rights reserved.
doi:10.1016/j.physd.2010.06.009

In the present work, we examine both sharp-interface and diffuse-interface models of gravity current motion in a heterogeneous porous medium. Our interest lies particularly in the homogenization of such models with respect to porous medium properties and in how the sharp-interface models can be recovered from the diffuse-interface models in the appropriate limits. Our previous work (Anderson et al. [7], hereafter denoted by AMM) on a related sharp-interface model describes the basic setting and motivation for our present investigation and so we outline those results below.

AMM examined homogenization of a gravity current that slumps in a heterogeneous porous medium along an impermeable boundary $z = 0$. They considered a single fluid model in which the free surface was defined as a sharp interface. They assumed that the background permeability of the porous medium was a given, rapidly varying function of space and pursued a homogenization theory for general two-dimensional geometries along with supporting computations valid in a slender gravity current limit for this nonlinear free boundary problem. While the asymptotic averaging of the bulk regions, where a linear elliptic equation applies, is relatively straightforward (e.g. [8]), the presence of a moving free boundary introduces nonlinearities as well as other complexities not addressed by the classical homogenization techniques. With an interface present, the model considered by AMM comprised a linear, variable coefficient elliptic equation in the bulk regions coupled to a kinematic (transport) equation evaluated at a moving interface. While there has been considerable effort in applying homogenization techniques to transport equations in bulk regions (e.g. E [9]), the transport equation of interest here is applied at a fluid interface within the region to be homogenized and has coefficients that are nonlocally coupled to the elliptic solve required to compute the flow. Bulk homogenization techniques rely on averaging quantities defined over volumes (or areas in two-dimensional applications) while the interfacial kinematic condition in a sharp-interface model applies on a surface (or curve in two-dimensional problems). The question then is how does one adapt homogenization techniques based on bulk averaging to handle the presence of a lower-dimensional dividing surface representing the interface between two fluid regions. As we describe in more detail below, AMM proposed an ad hoc 'pre-averaging' approach addressing this question; in the present work, we put this ad hoc approach on a more solid foundation through a rigorous derivation involving a diffuse-interface model.

The focus of the work in AMM was to address the complexities arising with homogenization and free boundaries. AMM addressed leading-order homogenization results in non-slender geometries for cases where the permeability function varied periodically in either one or two spatial directions. That is, they considered permeability functions of the form $K = K(X)$, $K = K(Z)$ or $K = K(X, Z)$ where $X = x/\epsilon$ and $Z = z/\epsilon$ are spatial variables associated with the rapid variation of the permeability in the limit when ϵ, a measure of the spatial variation of the permeability, is small. The focus was on configurations in which the free surface could be expressed as a single-valued function of space and time $z = h(x, t)$. Additionally, for the slender limit, in which the hydrostatic pressure approximation could be applied, and the case $K = K(X)$ they found both leading-order homogenization results as well as first-order corrections and compared these with numerical simulations of an evolution equation for the interface position h.

A central issue in the homogenization work of AMM involved the homogenization of the kinematic boundary condition [e.g. in the present work see (3)] governing the dynamics of the interface position $z = h(x, t)$. Two basic scenarios with respect to this equation arose corresponding to (I) permeability functions varying only in the horizontal direction [$K = K(X)$] and (II) permeability functions that have variation in the vertical direction [$K = K(Z)$ or $K = K(X, Z)$].

(I): When the background permeability varied only in the horizontal direction [i.e. $K = K(X)$] the quantities such as the horizontal and vertical velocity components (evaluated at the interface) appearing in Eq. (3) in general depend on x, t and, as in standard homogenization theory, also the fast space variable X. When one must decide how to homogenize this equation an approach that is similar to a classical one in a bulk region may be developed. This becomes more apparent in the slender geometry case in which Eq. (3) can be analytically reduced to a partial differential equation for $h(x, X, t)$. AMM examined this slender geometry situation in considerable detail and showed that leading-order homogenized solutions as well as first corrections to these solutions could be obtained. They found that the solution of the leading-order homogenized equations compared well with the numerical solution of the slender, variable media, problem; the difference between these two solutions was shown to scale linearly with ϵ. AMM also found that corrections to this leading-order homogenized solution agreed well with numerical simulations of the slender limit equations in the central portion of the gravity current away from the leading edge (or contact line); the difference between the corrected solution and the full numerical solution scaled with ϵ^2 in the interior region but scaled only linearly with ϵ near the leading edge. We comment that in this particular setting the contact line is itself a free boundary for the interface PDE and another level of homogenization at free boundaries must be addressed (a modified procedure that takes special care of the contact line regions in order to identify uniformly valid corrections is currently under investigation).

(II): In cases in which the background permeability field varies rapidly in both x and z directions AMM showed that a procedure involving an ad hoc 'pre-averaging' of the free surface condition (3) with respect to the vertical coordinate z, followed by a more standard homogenization procedure in the horizontal x direction, led to a closed set of homogenized equations (we outline this procedure in more detail below). Plausible arguments for this ad hoc procedure were given in AMM and indeed later numerical calculations[10] provided agreement between the leading-order homogenization results based on this averaging procedure and numerical simulations in the slender geometry limit for a doubly periodic background permeability.

Despite the apparent success of this 'pre-averaging' procedure adopted by AMM to allow for the homogenization of a free surface in a heterogeneous media, formal justification for its use is still lacking. That is, while the 'pre-averaging' procedure does yield a scaled-up system which is in mass conservative form, it is not mathematically clear how this is guaranteed in the averaging procedure. The purpose of the present work is to add improved mathematical and physical understanding of how this structure is preserved. In the present work, we examine an alternative, more rigorous, approach to the homogenization problem that we show leads to the same result as that obtained via the ad hoc pre-averaging. In particular, we shall examine a diffuse-interface model of a two-fluid gravity current problem where an interfacial region, characterized by continuously varying species and density fields and with thickness related to the scale of diffusion, replaces a mathematically sharp interface. In this context, a classical homogenization procedure can be applied without the complicating presence of a sharp interface. Then, once the leading-order homogenized system is obtained, we shall examine it in a sharp-interface limit (in the limit of vanishing solute diffusivity) to recover a homogenized, sharp-interface model directly from the homogenized diffuse-interface model. We shall demonstrate that this approach not only provides a homogenized diffuse-interface model but also provides independent justification of the homogenized, sharp-interface model obtained by AMM using the pre-averaging step.

Our work on the homogenization of these models is summarized schematically in Fig. 1. The sharp-interface two-fluid model is identified as Model 2. We interpret this model as one describing the dynamics of two immiscible fluids with diffusion coefficient $D = 0$.

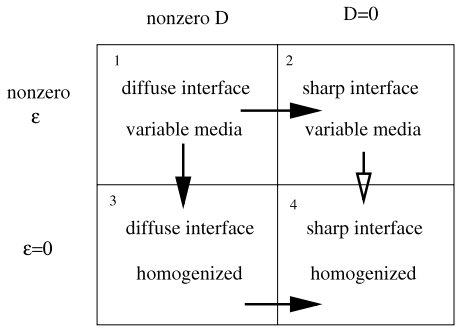

Fig. 1. Four descriptions for gravity current flow in porous media with rapidly varying medium properties. The left-side boxes (1 and 3) represent models with species diffusion and diffuse interfaces. The right-side boxes (2 and 4) represent sharp-interface models (e.g. AMM). Models 3 and 4 are obtained via homogenization from the variable media models 1 and 2, respectively. Models 2 and 4 are obtained via sharp-interface analysis of the diffuse-interface models 1 and 3, respectively.

As we outline in detail below, a homogenization procedure – using a pre-averaging step – represented by the limit $\epsilon \to 0$ leads to a set of leading-order homogenized equations identified as Model 4. Since the derivation of Model 4 via Model 2, represented by the open arrow, relies on an ad hoc pre-averaging step, we wish to justify Model 4 by deriving it from an alternate method. In particular, starting with a variable media, diffuse-interface problem identified as Model 1, we first apply a homogenization procedure taking $\epsilon \to 0$, which leads to the homogenized, diffuse-interface problem identified as Model 3. Since Model 1 and Model 3 do not involve explicit representation of an interfacial boundary, only standard homogenization theory is required. Then, we examine Model 3 in a sharp-interface limit characterized by $D \to 0$ in order to obtain Model 4. The derivation of Model 4 from Model 1 via Model 3, as indicated by solid arrows, thus relies on first homogenizing the diffuse-interface model via standard methods ($\epsilon \to 0$) and then examining a sharp-interface limit ($D \to 0$). This route to Model 4 does not involve pre-averaging a sharp-interface boundary condition. Additionally, we shall demonstrate that our sharp-interface analysis, which provides a connection between Model 3 and Model 4 also provides a similar connection between Model 1 and Model 2, closing the loop. Therefore, the passage from Model 1 to Model 4 via Model 2 can be interpreted as the limit $D \to 0$ followed by the limit $\epsilon \to 0$. The passage from Model 1 to Model 4 via Model 3 can be interpreted as the limit $\epsilon \to 0$ followed by the limit $D \to 0$.

The underlying assumptions built into the two routes from Model 1 to Model 4 are worth emphasis. The route via Model 3 describes a scenario in which the length scale of the permeability variations is assumed to be much smaller than the interface thickness (i.e. $\epsilon \to 0$ first, then $D \to 0$). On the other hand, the route via Model 2 describes a scenario in which the permeability variations are, by the nature of the sharp-interface model in which they are represented, much larger than the interface thickness (i.e. $D \to 0$ first, then $\epsilon \to 0$). The connection of these approaches to the homogenized, sharp-interface limit of Model 4 by these distinctly different routes is demonstrated in the present work.

The paper is organized as follows. In Section 2 we outline the sharp-interface two-fluid model and its homogenization based on the procedure implemented by AMM. This section extends the basic model of AMM, who addressed a one-fluid model, in order to allow a direct comparison between sharp-interface and diffuse-interface models. In Section 3 we describe a diffuse-interface model and its homogenization. In Section 4 we give a one-dimensional solution of the diffuse-interface model that reveals the structure of the solutions through the interfacial region. In Section 5 we examine the sharp-interface limit of the homogenized diffuse-interface model and show that it recovers the homogenized model from Section 2. Here we also point out that the sharp-interface limit connects the diffuse-interface model and sharp-interface model in the variable media setting as well. Conclusions are given in Section 6.

2. Sharp-interface, two-fluid model

We describe here the governing equations for two immiscible fluids in a spatially heterogeneous porous medium. The two fluid regions are coupled through interfacial boundary conditions applied at a 'sharp' interface (i.e. an interface with zero thickness). This description follows to some degree a second paper of Anderson et al. [10] in which they examined a two-fluid model but only for the case of uniform permeability. Here we outline the details of the two-fluid model and the homogenization approach of AMM for a spatially varying background permeability.

In fluid j ($j = 1, 2$), the governing equations are

$$\nabla \cdot \boldsymbol{u}^j = 0, \tag{1}$$

$$\boldsymbol{u}^j = -K(x/\epsilon, z/\epsilon)\left[\nabla p^j + \rho^j g \hat{\mathbf{k}}\right] = -K_c(x/\epsilon, z/\epsilon)\left[\nabla \phi^j + \Delta\rho^j \hat{\mathbf{k}}\right], \tag{2}$$

where $\boldsymbol{u}^j$ is the velocity vector, here taken to be two-dimensional with horizontal and vertical components u^j and w^j, respectively, p^j is the pressure in fluid j, $K = k/\mu$, where k is the permeability and μ is the viscosity (here assumed to be the same for both fluids), ρ^j is the (assumed constant) density in fluid j, g is gravitational acceleration and $\hat{\mathbf{k}}$ is a unit vector in the vertical direction. We have defined $\Delta\rho^j = \rho^j/\rho^* - 1$ where ρ^* is a reference density, $\phi^j = p^j/(\rho^* g) + z$ and $K_c = k\rho^* g/\mu$. The parameter ϵ, which is assumed to be small, measures the rapid spatial variation of the permeability.

The above equations are subject to a kinematic condition at the moving interface

$$\frac{\partial h}{\partial t} = -u^1 \frac{\partial h}{\partial x} + w^1 = -u^2 \frac{\partial h}{\partial x} + w^2 \quad \text{at } z = h(x, t), \tag{3}$$

and continuity of pressure $p^1 = p^2$ (or equivalently $\phi^1 = \phi^2$) at $z = h(x, t)$. While additional boundary and initial conditions would apply for a specific gravity current configuration [7,10], these will not fundamentally change the ideas applied in the present case and so we omit them here for simplicity.

We homogenize the above two-fluid model using a procedure analogous to that of AMM. We introduce fast spatial variables $X = x/\epsilon$ and $Z = z/\epsilon$ and treat x, X, z and Z as independent variables. We assume expansions for ϕ^j, u^j, w^j and h of the form

$$\phi^j = \phi_0^j(x, z, X, Z, t) + \epsilon\phi_1^j(x, z, X, Z, t) + \cdots, \tag{4}$$

$$u^j = u_0^j(x, z, X, Z, t) + \epsilon u_1^j(x, z, X, Z, t) + \cdots, \tag{5}$$

$$w^j = w_0^j(x, z, X, Z, t) + \epsilon w_1^j(x, z, X, Z, t) + \cdots, \tag{6}$$

$$h = h_0(x, X, t) + \epsilon h_1(x, X, t) + \cdots. \tag{7}$$

Following standard asymptotic homogenization methods (e.g. [8]) in which multiple space scales are introduced we write

$$\frac{\partial}{\partial x} \to \frac{\partial}{\partial x} + \frac{1}{\epsilon}\frac{\partial}{\partial X}, \qquad \frac{\partial}{\partial z} \to \frac{\partial}{\partial z} + \frac{1}{\epsilon}\frac{\partial}{\partial Z}. \tag{8}$$

An equation for ϕ^j can be obtained by combining Eqs. (1) and (2). With the above transformations we have

$$\left(\frac{\partial}{\partial x} + \frac{1}{\epsilon}\frac{\partial}{\partial X}\right)\left[K_c(X, Z)\left(\frac{\partial\phi^j}{\partial x} + \frac{1}{\epsilon}\frac{\partial\phi^j}{\partial X}\right)\right] + \left(\frac{\partial}{\partial z} + \frac{1}{\epsilon}\frac{\partial}{\partial Z}\right)\left[K_c(X, Z)\left(\frac{\partial\phi^j}{\partial z} + \Delta\rho^j + \frac{1}{\epsilon}\frac{\partial\phi^j}{\partial Z}\right)\right] = 0. \tag{9}$$

At $\mathcal{O}(\epsilon^{-2})$ we find $\mathcal{L}\phi_0^j = 0$ where $\mathcal{L}$ is a linear operator defined by

$$\mathcal{L} \equiv \frac{\partial}{\partial X}\left(K_c\frac{\partial}{\partial X}\right) + \frac{\partial}{\partial Z}\left(K_c\frac{\partial}{\partial Z}\right). \tag{10}$$

This is solved by taking $\phi_0^j = \phi_0^j(x, z, t)$ independent of the fast scales X and Z.

At $\mathcal{O}(\epsilon^{-1})$ we find that

$$\frac{\partial}{\partial X}\left[K_c\left(\frac{\partial\phi_0^j}{\partial x} + \frac{\partial\phi_1^j}{\partial X}\right)\right] + \frac{\partial}{\partial Z}\left[K_c\left(\frac{\partial\phi_0^j}{\partial z} + \Delta\rho^j + \frac{\partial\phi_1^j}{\partial Z}\right)\right] = 0, \tag{11}$$

or in terms of $\mathcal{L}$

$$\mathcal{L}\phi_1^j = -\frac{\partial K_c}{\partial X}\frac{\partial\phi_0^j}{\partial x} - \frac{\partial K_c}{\partial Z}\left(\frac{\partial\phi_0^j}{\partial z} + \Delta\rho^j\right). \tag{12}$$

The solution to Eq. (12) can be expressed as

$$\phi_1^j = \theta_1(X, Z)\frac{\partial\phi_0^j}{\partial x} + \theta_2(X, Z)\left(\frac{\partial\phi_0^j}{\partial z} + \Delta\rho^j\right), \tag{13}$$

where the coefficients θ_1 and θ_2 satisfy the two cell problems [11] on [0, 1] and [0, 1]

$$\mathcal{L}\theta_1 = -\frac{\partial K_c}{\partial X}, \qquad \mathcal{L}\theta_2 = -\frac{\partial K_c}{\partial Z}. \tag{14}$$

At $\mathcal{O}(1)$ we find, upon integrating the governing equations in X and Z, that ϕ_0^j satisfies the general elliptic problem

$$\nabla\cdot\left(\mathbf{K}_{eff}\cdot\nabla\phi_0^j\right) = \alpha\frac{\partial^2\phi_0^j}{\partial x^2} + 2\beta\frac{\partial^2\phi_0^j}{\partial x\partial z} + \gamma\frac{\partial^2\phi_0^j}{\partial z^2} = 0, \tag{15}$$

where

$$\mathbf{K}_{eff} = \begin{bmatrix}\alpha & \beta\\ \beta & \gamma\end{bmatrix}, \tag{16}$$

and the coefficients are given by

$$\alpha = \langle\langle K_c\rangle\rangle - \langle\langle K_c|\nabla\theta_1|^2\rangle\rangle, \tag{17}$$

$$\beta = -\langle\langle K_c\nabla\theta_1\cdot\nabla\theta_2\rangle\rangle, \tag{18}$$

$$\gamma = \langle\langle K_c\rangle\rangle - \langle\langle K_c|\nabla\theta_2|^2\rangle\rangle, \tag{19}$$

where $\langle\langle\cdot\rangle\rangle = \int_0^1\int_0^1\cdot\,\mathrm{d}X\mathrm{d}Z$.

We now address the boundary condition (3). We follow here the ad hoc 'pre-averaging' of this boundary condition as outlined in AMM. That is, we formally 'pre-average' equation (3) to obtain

$$\frac{\partial h}{\partial t} = -\langle u^1\rangle_Z\frac{\partial h}{\partial x} + \langle w^1\rangle_Z = -\langle u^2\rangle_Z\frac{\partial h}{\partial x} + \langle w^2\rangle_Z \quad \text{at } z = h(x, X, t), \tag{20}$$

where $\langle\cdot\rangle_Z$ denotes an average in Z so that these quantities depend only on the variables x, X and t. As outlined in the introduction, our objective is now to justify the use of this pre-averaging by showing that it agrees with results obtained by taking the sharp-interface limit of a homogenized diffuse-interface model.

We insert the expansion for h into Eq. (20) and collect powers of ϵ. At $\mathcal{O}(\epsilon^{-1})$ the boundary conditions are satisfied by taking $h_0 = h_0(x,t)$. At $\mathcal{O}(1)$ the boundary conditions can be written

$$\frac{\partial h_0}{\partial t} = -\langle u_0^1\rangle_Z\left(\frac{\partial h_0}{\partial x}+\frac{\partial h_1}{\partial X}\right)+\langle w_0^1\rangle_Z = -\langle u_0^2\rangle_Z\left(\frac{\partial h_0}{\partial x}+\frac{\partial h_1}{\partial X}\right)+\langle w_0^2\rangle_Z. \tag{21}$$

Averaging this in X gives

$$\begin{aligned}\frac{\partial h_0}{\partial t} &= -\langle\langle u_0^1\rangle_Z\rangle_X\frac{\partial h_0}{\partial x}+\left\langle\left\langle K_c\left(\frac{\partial\phi_0^1}{\partial x}+\frac{\partial\phi_1^1}{\partial X}\right)\right\rangle_Z\frac{\partial h_1}{\partial X}\right\rangle_X+\langle\langle w_0^1\rangle_Z\rangle_X\\ &= -\langle\langle u_0^2\rangle_Z\rangle_X\frac{\partial h_0}{\partial x}+\left\langle\left\langle K_c\left(\frac{\partial\phi_0^2}{\partial x}+\frac{\partial\phi_1^2}{\partial X}\right)\right\rangle_Z\frac{\partial h_1}{\partial X}\right\rangle_X+\langle\langle w_0^2\rangle_Z\rangle_X.\end{aligned} \tag{22}$$

From the equations in the bulk we know that the leading-order velocity components are

$$u_0^j(x,z,X,Z) = -K_c(X,Z)\left(\frac{\partial\phi_0^j}{\partial x}+\frac{\partial\phi_1^j}{\partial X}\right), \tag{23}$$

$$w_0^j(x,z,X,Z) = -K_c(X,Z)\left(\frac{\partial\phi_0^j}{\partial z}+\Delta\rho^j+\frac{\partial\phi_1^j}{\partial Z}\right), \tag{24}$$

for $j=1,2$. We can integrate by parts and use Eq. (11) to show that, as in AMM, the following term vanishes,

$$\begin{aligned}\left\langle\left\langle K_c\left(\frac{\partial\phi_0^j}{\partial x}+\frac{\partial\phi_1^j}{\partial X}\right)\right\rangle_Z\frac{\partial h_1}{\partial X}\right\rangle_X &= -\left\langle h_1\frac{\partial}{\partial X}\left\langle K_c\left(\frac{\partial\phi_0^j}{\partial x}+\frac{\partial\phi_1^j}{\partial X}\right)\right\rangle_Z\right\rangle_X,\\ &= -\left\langle h_1\left\langle\frac{\partial}{\partial X}\left[K_c\left(\frac{\partial\phi_0^j}{\partial x}+\frac{\partial\phi_1^j}{\partial X}\right)\right]\right\rangle_Z\right\rangle_X,\\ &= \left\langle h_1\left\langle\frac{\partial}{\partial Z}\left[K_c\left(\frac{\partial\phi_0^j}{\partial z}+\Delta\rho^j+\frac{\partial\phi_1^j}{\partial Z}\right)\right]\right\rangle_Z\right\rangle_X,\\ &= \left\langle h_1\left[K_c\left(\frac{\partial\phi_0^j}{\partial z}+\Delta\rho^j+\frac{\partial\phi_1^j}{\partial Z}\right)\right]_{Z=0}^{Z=1}\right\rangle_X = 0.\end{aligned} \tag{25}$$

The full set of averaged leading-order equations are

$$\nabla\cdot\langle\langle\boldsymbol{u}_0^j\rangle\rangle = 0, \tag{26}$$

$$\langle\langle\boldsymbol{u}_0^j\rangle\rangle = -\mathbf{K}_{eff}\cdot\left(\nabla\phi_0^j+\Delta\rho^j\hat{\mathbf{k}}\right), \tag{27}$$

for $j=1,2$, subject to the free surface boundary conditions

$$\frac{\partial h_0}{\partial t} = -\langle\langle u_0^1\rangle\rangle\frac{\partial h_0}{\partial x}+\langle\langle w_0^1\rangle\rangle = -\langle\langle u_0^2\rangle\rangle\frac{\partial h_0}{\partial x}+\langle\langle w_0^2\rangle\rangle \quad \text{at } z=h_0(x,t), \tag{28}$$

$$\phi_0\,|_-^+ = 0, \quad \text{at } z=h_0(x,t). \tag{29}$$

Note that the free surface condition can also be expressed more generally as $\boldsymbol{u}_0^1\cdot\hat{\mathbf{n}} = \boldsymbol{u}_0^2\cdot\hat{\mathbf{n}} = \boldsymbol{v}_I\cdot\hat{\mathbf{n}}$, where $\hat{\mathbf{n}}$ is a unit normal vector to the interface.

These results will now be compared with results obtained from an alternative gravity current model in which the sharp interface is replaced by continuously varying species and density fields. More specifically, we shall show that this same homogenized sharp-interface model can be derived by first homogenizing a diffuse-interface model and then taking its sharp-interface limit.

3. Gravity current with species diffusion

A model for the flow of a (miscible) brine solution in porous media is made up of a mass balance condition, a Darcy equation for the fluid flow and a diffusion equation for the species. In particular,

$$\frac{\partial(\chi\rho)}{\partial t}+\nabla\cdot(\chi\rho\boldsymbol{u}) = 0, \tag{30}$$

$$\frac{\partial(\chi\rho s)}{\partial t}+\nabla\cdot(\chi\rho s\boldsymbol{u}) = \nabla\cdot(\chi\rho\mathbf{D}\cdot\nabla s), \tag{31}$$

$$\boldsymbol{u} = -\mathbf{K}\cdot\left(\nabla p+\rho g\hat{\mathbf{k}}\right), \tag{32}$$

where we take as an equation of state

$$\rho = \rho^* f(s). \tag{33}$$

Here χ is the porosity, which for simplicity we take to be constant, ρ is the fluid density, $\boldsymbol{u}$ is the fluid velocity, s is the species mass fraction, $\mathbf{D}$ is a dispersion tensor which accounts for both Fickian diffusion and mechanical dispersion, which we take to be constant (in general $\mathbf{D}$ is a symmetric tensor and a function of $\boldsymbol{u}$), $\mathbf{K}$ is a tensor which for our purposes here we assume to have the form $K\mathbf{I}$, where $K = k/\mu$ is a scalar function, k is the permeability and μ is the viscosity. We assume that K is a prescribed function of space. In the equation of state ρ^* is a reference density and $f(s)$ is a dimensionless function to be specified. For dense brine solutions, the viscosity can be a strong function of species mass fraction [12], although for simplicity we take it to be constant.

With χ constant, the scalar permeability function and the field variable $\phi = p/(\rho^* g) + z$ these equations can be reduced to

$$\frac{\partial \rho}{\partial t} + \nabla \cdot (\rho \boldsymbol{u}) = 0, \tag{34}$$

$$\frac{\partial (\rho s)}{\partial t} + \nabla \cdot (\rho s \boldsymbol{u}) = \nabla \cdot (\rho \mathbf{D} \cdot \nabla s)\,, \tag{35}$$

$$\boldsymbol{u} = -K_c \left[\nabla \phi + (f(s) - 1)\hat{\mathbf{k}} \right], \tag{36}$$

where $K_c = k\rho^* g/\mu$.

We now assume that $K_c = K_c(X, Z)$ where $X = x/\epsilon$ and $Z = z/\epsilon$ with ϵ a small parameter and seek a solution as expansions of the form

$$\phi = \phi_0(x, z, X, Z, t) + \epsilon \phi_1(x, z, X, Z, t) + \cdots, \tag{37}$$

etc. The homogenization procedure uses a multiple scale analysis in which the derivatives transform as before in Eq. (8). The equations in expanded form are

$$\frac{\partial \rho}{\partial t} = \left(\frac{\partial}{\partial x} + \frac{1}{\epsilon}\frac{\partial}{\partial X} \right) \left[\rho K_c(X, Z) \left(\frac{\partial \phi}{\partial x} + \frac{1}{\epsilon}\frac{\partial \phi}{\partial X} \right) \right] + \left(\frac{\partial}{\partial z} + \frac{1}{\epsilon}\frac{\partial}{\partial Z} \right) \left[\rho K_c(X, Z) \left(\frac{\partial \phi}{\partial z} + \frac{1}{\epsilon}\frac{\partial \phi}{\partial Z} + f(s) - 1 \right) \right] \tag{38}$$

$$\begin{aligned} \frac{\partial (\rho s)}{\partial t} &= \left(\frac{\partial}{\partial x} + \frac{1}{\epsilon}\frac{\partial}{\partial X} \right) \left[\rho s K_c \left(\frac{\partial \phi}{\partial x} + \frac{1}{\epsilon}\frac{\partial \phi}{\partial X} \right) \right] + \left(\frac{\partial}{\partial z} + \frac{1}{\epsilon}\frac{\partial}{\partial Z} \right) \left[\rho s K_c \left(\frac{\partial \phi}{\partial z} + \frac{1}{\epsilon}\frac{\partial \phi}{\partial Z} + f(s) - 1 \right) \right] \\ &\quad + \left(\frac{\partial}{\partial x} + \frac{1}{\epsilon}\frac{\partial}{\partial X} \right) \left\{ \rho \left[D_{11} \left(\frac{\partial s}{\partial x} + \frac{1}{\epsilon}\frac{\partial s}{\partial X} \right) + D_{12} \left(\frac{\partial s}{\partial z} + \frac{1}{\epsilon}\frac{\partial s}{\partial Z} \right) \right] \right\}, \\ &\quad + \left(\frac{\partial}{\partial z} + \frac{1}{\epsilon}\frac{\partial}{\partial Z} \right) \left\{ \rho \left[D_{21} \left(\frac{\partial s}{\partial x} + \frac{1}{\epsilon}\frac{\partial s}{\partial X} \right) + D_{22} \left(\frac{\partial s}{\partial z} + \frac{1}{\epsilon}\frac{\partial s}{\partial Z} \right) \right] \right\}. \end{aligned} \tag{39}$$

At $\mathcal{O}(\epsilon^{-2})$ we find

$$0 = \frac{\partial}{\partial X} \left(\rho_0 K_c \frac{\partial \phi_0}{\partial X} \right) + \frac{\partial}{\partial Z} \left(\rho_0 K_c \frac{\partial \phi_0}{\partial Z} \right), \tag{40}$$

$$0 = \frac{\partial}{\partial X} \left(\rho_0 s_0 K_c \frac{\partial \phi_0}{\partial X} \right) + \frac{\partial}{\partial Z} \left(\rho_0 s_0 K_c \frac{\partial \phi_0}{\partial Z} \right) + \frac{\partial}{\partial X} \left[\rho_0 \left(D_{11} \frac{\partial s_0}{\partial X} + D_{12} \frac{\partial s_0}{\partial Z} \right) \right] + \frac{\partial}{\partial Z} \left[\rho_0 \left(D_{21} \frac{\partial s_0}{\partial X} + D_{22} \frac{\partial s_0}{\partial Z} \right) \right]. \tag{41}$$

These are solved by functions $\phi_0 = \phi_0(x, z, t)$, $s_0 = s_0(x, z, t)$ (and hence $\rho_0 = \rho_0(x, z, t)$) that are independent of the fast scales X and Z. These forms lead us to define a second operator $\mathcal{L}^D$, analogous to $\mathcal{L}$ in Eq. (10), by

$$\mathcal{L}^D \equiv \frac{\partial}{\partial X} \left(D_{11} \frac{\partial}{\partial X} + D_{12} \frac{\partial}{\partial Z} \right) + \frac{\partial}{\partial Z} \left(D_{21} \frac{\partial}{\partial X} + D_{22} \frac{\partial}{\partial Z} \right). \tag{42}$$

At $\mathcal{O}(\epsilon^{-1})$ we find that

$$\rho_0 \mathcal{L} \phi_1 = -\rho_0 \left[\frac{\partial \phi_0}{\partial x} \frac{\partial K_c}{\partial X} + \left(\frac{\partial \phi_0}{\partial z} + f(s_0) - 1 \right) \frac{\partial K_c}{\partial Z} \right], \tag{43}$$

$$\rho_0 s_0 \mathcal{L} \phi_1 + \rho_0 \mathcal{L}^D s_1 = -\rho_0 s_0 \left[\frac{\partial \phi_0}{\partial x} \frac{\partial K_c}{\partial X} + \left(\frac{\partial \phi_0}{\partial z} + f(s_0) - 1 \right) \frac{\partial K_c}{\partial Z} \right]. \tag{44}$$

The second of these reduces simply to $\mathcal{L}^D s_1 = 0$ upon using the first equation. These equations are solved by taking $s_1 = s_1(x, z, t)$ and

$$\phi_1 = \theta_1(X, Z) \frac{\partial \phi_0}{\partial x} + \theta_2(X, Z) \left(\frac{\partial \phi_0}{\partial z} + f(s_0) - 1 \right), \tag{45}$$

where the coefficients θ_1 and θ_2 satisfy the two cell problems (14) identified in the previous section.

At $\mathcal{O}(1)$ we can write down the equations, average them in X and Z, and use

$$\left\langle\!\left\langle K_c \frac{\partial \theta_1}{\partial X} \right\rangle\!\right\rangle = -\langle\!\langle K_c |\nabla \theta_1|^2 \rangle\!\rangle, \tag{46}$$

$$\left\langle\!\left\langle K_c \frac{\partial \theta_1}{\partial Z} \right\rangle\!\right\rangle = \left\langle\!\left\langle K_c \frac{\partial \theta_2}{\partial X} \right\rangle\!\right\rangle = -\langle\!\langle K_c \nabla \theta_1 \cdot \nabla \theta_2 \rangle\!\rangle, \tag{47}$$

$$\left\langle\!\left\langle K_c \frac{\partial \theta_2}{\partial Z} \right\rangle\!\right\rangle = -\langle\!\langle K_c |\nabla \theta_2|^2 \rangle\!\rangle, \tag{48}$$

where $\langle\!\langle \cdot \rangle\!\rangle = \int_0^1 \int_0^1 \cdot \, \mathrm{d}X \mathrm{d}Z$ to find that the leading-order homogenized equations are

$$\frac{\partial \rho_0}{\partial t} + \nabla \cdot (\rho_0 \boldsymbol{u}_0) = 0, \tag{49}$$

$$\frac{\partial (\rho_0 s_0)}{\partial t} + \nabla \cdot (\rho_0 s_0 \boldsymbol{u}_0) = \nabla \cdot (\rho_0 \mathbf{D} \cdot \nabla s_0), \tag{50}$$

$$\boldsymbol{u}_0 = -\mathbf{K}_{\mathit{eff}} \cdot \left[\nabla \phi_0 + (f(s_0) - 1)\hat{\mathbf{k}} \right], \tag{51}$$

where $\mathbf{K}_{\mathit{eff}}$ is given in Eqs. (16)–(19).

We note here that the above homogenization procedure has been applied to a system in which the interfacial region between the two phases is defined implicitly, rather than explicitly as in the sharp-interface formulation of AMM. With the leading-order homogenized equations thus obtained, we shall investigate a sharp-interface limit of these equations in order to derive an associated sharp-interface model that can be compared directly to the leading-order homogenized results of AMM.

4. One-dimensional solution of diffusion-based model

The sharp-interface limit to be performed in the next section on the homogenized model above requires a clear understanding of the structure through and thickness of the interfacial region. For a classical diffusion equation it is well known that such a diffusive region has a thickness that scales with $\sqrt{Dt}$. The present context includes species diffusion coupled to a variable nonlinear density field and fluid flow. The general context is one in which we examine the limit $\epsilon \to 0$ (homogenization) before the limit of vanishing diffusivity $D \to 0$. In other words, the case under consideration has permeability variations (measured by ϵ) on a much smaller scale than that of the interfacial thickness (measured by D). The calculations below highlight the hydrodynamic effects of diffusion in the interfacial region and demonstrate that the interfacial thickness scaling $\sqrt{Dt}$ still holds.

Consider for simplicity the case with $\mathbf{K} = K\mathbf{I}$ and $\mathbf{D} = D\mathbf{I}$ where

$$\frac{\partial \rho}{\partial t} + \frac{\partial (\rho w)}{\partial z} = 0, \tag{52}$$

$$\frac{\partial (\rho s)}{\partial t} + \frac{\partial (\rho s w)}{\partial z} = D \frac{\partial}{\partial z} \left(\rho \frac{\partial s}{\partial z} \right), \tag{53}$$

$$w = -K \left(\frac{\partial p}{\partial z} + \rho g \right), \tag{54}$$

where $\rho = \rho^* f(s)$. We shall consider the case in which the mass fraction s attains constant values s^+ and s^- in the far-field ($z \to \pm\infty$) and where the fluid velocity vanishes as $z \to -\infty$. The fluid velocity in the far-field $z \to \infty$ remains to be determined in accordance with conservation of mass. Initial conditions correspond to an upper layer ($z > 0$) with mass fraction s^+ and a lower layer ($z < 0$) with mass fraction s^-. These conditions represent two layers initially separated that mix diffusively inside of a container closed at the bottom and open at the top. Here, the bulk fluid below the interfacial region is expected to be motionless while the bulk fluid above the interfacial region will experience a uniform flow due to volume change associated with the diffusion process occurring in the interfacial region.

We first note that Eq. (54) determines the pressure and is decoupled from Eqs. (52) and (53). Making use of $\rho = \rho^* f(s)$ we can write Eqs. (52) and (53) as

$$f'(s) \left[\frac{\partial s}{\partial t} + w \frac{\partial s}{\partial z} \right] + f(s) \frac{\partial w}{\partial z} = 0, \tag{55}$$

$$f(s) \left[\frac{\partial s}{\partial t} + w \frac{\partial s}{\partial z} \right] = D \frac{\partial}{\partial z} \left[f(s) \frac{\partial s}{\partial z} \right]. \tag{56}$$

Eqs. (55) and (56) can be solved by introducing the similarity transformation

$$\eta = \frac{z}{2\sqrt{Dt}}, \qquad w = \frac{Q(\eta)}{2\sqrt{Dt}}. \tag{57}$$

Transforming the derivatives in the standard way

$$\frac{\partial}{\partial t} \to -\frac{\eta}{2t} \frac{\mathrm{d}}{\mathrm{d}\eta}, \qquad \frac{\partial}{\partial z} \to \frac{1}{2\sqrt{Dt}} \frac{\mathrm{d}}{\mathrm{d}\eta}, \tag{58}$$

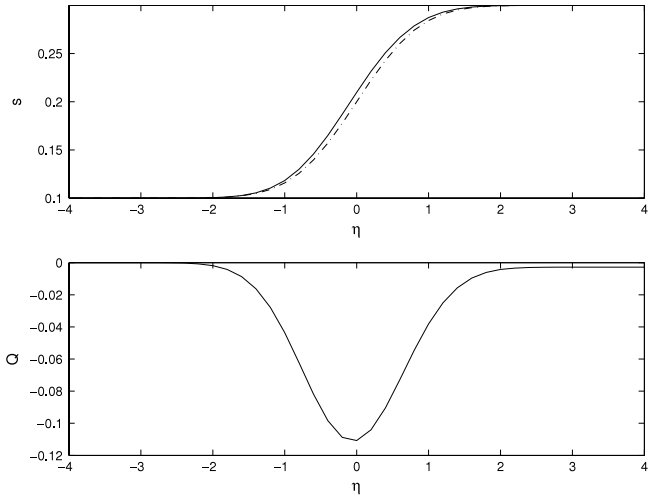

Fig. 2. This figure shows the numerically computed species profile, s and velocity function Q for the density function given by Eq. (61). Here $s^+ = 0.3$, $s^- = 0.1$, $L_P = 16$ and $L_M = -16$ and $N = 160$.

leads to a pair of ordinary differential equations for s and Q

$$\frac{\mathrm{d}}{\mathrm{d}\eta}\left[f(s)\frac{\mathrm{d}s}{\mathrm{d}\eta}\right] + f(s)(2\eta - Q)\frac{\mathrm{d}s}{\mathrm{d}\eta} = 0, \tag{59}$$

$$f(s)\frac{\mathrm{d}Q}{\mathrm{d}\eta} - f'(s)(2\eta - Q)\frac{\mathrm{d}s}{\mathrm{d}\eta} = 0. \tag{60}$$

These equations are subject to boundary conditions $s \to s^+$ as $\eta \to \infty$ and $s \to s^-$ and $Q \to 0$ as $\eta \to -\infty$.

We have examined the solution of (59) and (60) numerically on a finite interval $L_M < \eta < L_P$. This interval was discretized into N equal subintervals, the ODEs were discretized and the resulting system of nonlinear equations solved in two different ways for purposes of validation: a standard Newton's method and Matlab's `fsolve` command. The values of L_M, L_P and N were chosen so that the solution structure through the interfacial region was independent of these numerical parameters.

Fig. 2 shows the numerical solution of Eq. (59) and (60) for the nonlinear density function $f(s)$ given by

$$f(s) = 0.8319s^3 + 0.4958s^2 + 0.8417s + 0.9982, \tag{61}$$

where $\rho^* = 1\ \mathrm{g\ cm^{-3}}$. The species mass fraction connects smoothly through an interfacial region between the far-field values s^+ and s^-. The lower fluid layer is stagnant while a uniform flow towards the interfacial region occurs in the upper fluid layer. Within the interfacial region, the magnitude of the flow reaches a maximum. The diffusion of species gives rise to a change in fluid density and the corresponding volume change creates a local flow in the interfacial region as well as the spatially uniform flow in the upper bulk layer. Here $Q \to -0.0028$ as $\eta \to \infty$.

An approximate analytical representation of this structure can be obtained for a linear density function $f(s) = 1 + as$ in the limit $a \to 0$ (details are given in Appendix A). We find that the leading-order species profile satisfies a standard linear diffusion equation and has solution

$$s = s^- + \frac{1}{2}(s^+ - s^-)[1 + \mathrm{erf}(\eta)] + O(a). \tag{62}$$

Fig. 2 shows this solution (dashed line) in the upper plot; on the scale shown this line is nearly coincident with the full numerical solution with a nonlinear density (solid line). The corresponding flow is

$$Q = -\frac{a(s^+ - s^-)}{\sqrt{\pi}}\mathrm{e}^{-\eta^2} + O(a^2), \tag{63}$$

which shows that to leading-order in a, the flow is localized in the interfacial region. A far-field flow ($\eta \to \infty$) scales with a^2 and can be expressed as

$$Q(\eta \to \infty) = -\sqrt{\frac{2}{\pi}}(s^+ - s^-)^2 a^2 + \cdots. \tag{64}$$

This diffusion-driven volume change flow is towards the interfacial region regardless of the sign of the jump in species mass fraction across the interface.

A key feature of these solutions for either the linear or nonlinear density function, at least in terms of the sharp-interface analysis to follow, is that the thickness of the interfacial region l_i scales with $\sqrt{Dt}$. Therefore, for finite time, $l_i \to 0$ as $D \to 0$. Furthermore, the diffusive flux

$$D\frac{\partial s}{\partial z} \sim D\frac{1}{\sqrt{Dt}}\frac{\partial s}{\partial \eta} \sim \sqrt{D/t} \to 0 \tag{65}$$

in the limit $D \to 0$ for finite time. We shall incorporate this scaling information into the sharp-interface analysis given below.

5. Sharp-interface limit of diffusion-based model

The sharp-interface limit of Eqs. (49)–(51) can be obtained following procedures similar to those used in analysis of phase-field models. We shall adopt a 'pillbox' approach (see for example the sharp-interface analysis described in [13]) although an approach that specifically introduces surface-fitted coordinates (e.g. [14]) and generates inner and outer solutions to these equations via matched asymptotic expansions is also possible (see for example [15]).

In the following analysis, we shall assume that the dispersion tensor can be written $\mathbf{D} = D\boldsymbol{\mathcal{D}}$ where D is a scalar diffusion coefficient representative of the scale of $\mathbf{D}$ and $\boldsymbol{\mathcal{D}}$ is an $O(1)$ tensor. In particular, we wish to examine Eqs. (49)–(51) in the limit $D \to 0$.

In an effort to streamline the notation as much as possible we shall restate Eqs. (49)–(51) by dropping the subscript '0' from the original homogenization expansion. We then have for the leading-order homogenized problem for the diffusion-based model the equations

$$\frac{\partial \rho}{\partial t} + \nabla \cdot (\rho \boldsymbol{u}) = 0, \tag{66}$$

$$\frac{\partial (\rho s)}{\partial t} + \nabla \cdot (\rho s \boldsymbol{u}) = D \nabla \cdot (\rho \boldsymbol{\mathcal{D}} \cdot \nabla s)\,, \tag{67}$$

$$\boldsymbol{u} = -\mathbf{K}_{\mathit{eff}} \cdot \left[\nabla \phi + (f(s) - 1)\hat{\mathbf{k}} \right]. \tag{68}$$

As observed in the analysis and solution of the one-dimensional problem in the previous section, the thickness of the diffusive interfacial region scales with $l_i \sim \sqrt{Dt}$. For sufficiently large times, the diffuse-interface thickness will reach the size of any finite size container even for cases with small solute diffusion. Our interest here is to extract the sharp-interface limit of the above equations for finite time scenarios; that is, $l_i \to 0$ as $D \to 0$.

Away from such a thin interfacial region the system is in one of two bulk regions characterized by uniform densities $\rho^{\pm}$ and species mass fraction $s^{\pm}$ such as would be the case for the (finite time) evolution of a dense brine system surrounded by water. We assume that $\rho^{\pm}$ and $s^{\pm}$ are constants. Under these assumptions, the leading-order equations that follow from Eqs. (66)–(68) for the two bulk fluid regions are

$$\nabla \cdot \boldsymbol{u}_0^j = 0, \tag{69}$$

$$\boldsymbol{u}_0^j = -\mathbf{K}_{\mathit{eff}} \cdot \left[\nabla \phi_0^j + (f(s_0^j) - 1)\hat{\mathbf{k}} \right]. \tag{70}$$

The corresponding interfacial jump conditions that couple these bulk equations are now obtained by examining each of the governing equations in turn.

Continuity equation: We apply a standard pillbox argument (e.g. [13]) first to the continuity equation (66)

$$\frac{\partial \rho}{\partial t} + \nabla \cdot (\rho \boldsymbol{u}) = 0. \tag{71}$$

Integrating this equation over a pillbox of volume $\mathcal{V}$ attached to the interface and using the divergence theorem and the transport theorem gives

$$\frac{\mathrm{d}}{\mathrm{d}t} \int_{\mathcal{V}} \rho \mathrm{d}V - \int_{\mathcal{S}} \rho \boldsymbol{v}_I \cdot \hat{\mathbf{n}} \mathrm{d}S + \int_{\mathcal{S}} \rho \boldsymbol{u} \cdot \hat{\mathbf{n}} \mathrm{d}S = 0 \tag{72}$$

where $\boldsymbol{v}_I$ is the interface velocity vector.

The volume integral term vanishes in the limit of $\mathcal{V} \to 0$ since the time variation of the total mass in the volume is bounded. This then gives

$$\int_{\mathcal{S}} \rho (\boldsymbol{u} - \boldsymbol{v}_I) \cdot \hat{\mathbf{n}} \mathrm{d}S = 0. \tag{73}$$

Arguing that the contributions from the sides of the pillbox vanish and that the interfacial region contained by the pillbox can be chosen arbitrarily leads to the standard mass continuity condition

$$\rho (\boldsymbol{u} - \boldsymbol{v}_I) \cdot \hat{\mathbf{n}} \,|_{-}^{+} = 0. \tag{74}$$

We define a mass flux $J = \rho^1 (\boldsymbol{u}^1 - \boldsymbol{v}_I) \cdot \hat{\mathbf{n}} = \rho^2 (\boldsymbol{u}^2 - \boldsymbol{v}_I) \cdot \hat{\mathbf{n}}$ so that this condition requires continuity of mass flux, $J\,|_{-}^{+} = 0$.

Species Diffusion Equation: We next apply a similar pillbox approach to the species diffusion equation (67)

$$\frac{\partial (\rho s)}{\partial t} + \nabla \cdot (\rho s \boldsymbol{u}) = D \nabla \cdot (\rho \boldsymbol{\mathcal{D}} \cdot \nabla s)\,. \tag{75}$$

Integrating this equation over the pillbox, applying the divergence theorem and transport theorem gives

$$\frac{\mathrm{d}}{\mathrm{d}t} \int_{\mathcal{V}} \rho s \mathrm{d}V - \int_{\mathcal{S}} \rho s \boldsymbol{v}_I \cdot \hat{\mathbf{n}} \mathrm{d}S + \int_{\mathcal{S}} \rho s \boldsymbol{u} \cdot \hat{\mathbf{n}} \mathrm{d}S = D \int_{\mathcal{S}} \rho (\boldsymbol{\mathcal{D}} \cdot \nabla s) \cdot \hat{\mathbf{n}} \mathrm{d}S. \tag{76}$$

Again the volume integral vanishes in the limit $\mathcal{V} \to 0$ since the time variation of the integral ρs is bounded. Then, since diffusive flux $D \nabla s \to 0$ as $D \to 0$ (see Section 4) one obtains

$$\rho s (\boldsymbol{u} - \boldsymbol{v}_I) \cdot \hat{\mathbf{n}} \,|_{-}^{+} = 0. \tag{77}$$

In terms of the mass flux J, noting that $J\,|_-^+ = 0$ we have

$$J\left(s\,|_-^+\right) = 0. \tag{78}$$

Now, since the jump in species fraction s is nonzero, this condition can be satisfied only if $J = 0$. That is, in this limit, the interface is a material interface where

$$\boldsymbol{u}^1 \cdot \hat{\mathbf{n}} = \boldsymbol{u}^2 \cdot \hat{\mathbf{n}} = \boldsymbol{v}_I \cdot \hat{\mathbf{n}}. \tag{79}$$

Darcy Equation: Finally, we apply the pillbox argument to the Darcy equation

$$\boldsymbol{u} = -\mathbf{K} \cdot \left[\nabla\phi + (f(s) - 1)\hat{\mathbf{k}}\right], \tag{80}$$

where we will interpret $\mathbf{K}$ as either the constant $\mathbf{K}_{eff}$ in the homogenized diffuse-interface model [see Eq. (68)] or a variable permeability that could depend on $X = x/\epsilon$ and/or $Z = z/\epsilon$ [e.g. as in Eq. (32) or (36)]. Integrating over the pillbox volume $\mathcal{V}$ gives

$$\int_{\mathcal{V}} \boldsymbol{u}\mathrm{d}V = -\int_{\mathcal{V}} \mathbf{K} \cdot \nabla\phi \mathrm{d}V - \int_{\mathcal{V}} (f(s) - 1)\mathbf{K} \cdot \hat{\mathbf{k}}\mathrm{d}V. \tag{81}$$

The first and third integrals in this expression have bounded integrands and consequently as $\mathcal{V} \to 0$ these integrals vanish. The remaining expression gives

$$\begin{aligned} 0 &= \int_{\mathcal{V}} \mathbf{K} \cdot \nabla\phi \mathrm{d}V \\ &= \int_{\mathcal{V}} \left[\nabla \cdot (\mathbf{K}\phi) - \phi\nabla \cdot \mathbf{K}\right] \mathrm{d}V, \\ &= \int_{\mathcal{S}} \phi\mathbf{K} \cdot \hat{\mathbf{n}}\mathrm{d}S - \int_{\mathcal{V}} \phi\nabla \cdot \mathbf{K}\mathrm{d}V. \end{aligned} \tag{82}$$

In the case where $\mathbf{K} = \mathbf{K}_{eff}$ is constant, such as in the homogenized, diffuse-interface problem of Model 3 the last volume integral in the above expression vanishes. It follows that the jump in ϕ across the interface is zero

$$\phi\,|_-^+ = 0. \tag{83}$$

If instead we had examined the variable media, diffuse-interface model in which the permeability was a function of fast variables $\mathbf{K} = \mathbf{K}(x/\epsilon, z/\epsilon)$ (i.e. Model 1), the term $\nabla \cdot \mathbf{K}$ would be nonzero in general and would scale with $1/\epsilon$. However, in this case the volume integral in the last expression in Eq. (82) would scale with l_i/ϵ and hence would vanish in the sharp-interface limit $l_i \to 0$ with fixed $\epsilon > 0$. The result would suggest that

$$\phi\mathbf{K} \cdot \hat{\mathbf{n}}\,|_-^+ = 0. \tag{84}$$

If $\mathbf{K}$ is continuous across the interface we would again recover the interfacial jump condition (83).

Summarizing the above results, we find that the homogenized diffuse-interface model (i.e. Model 3) reduces in the sharp-interface limit to Eqs. (69) and (70) in the two bulk regions subject to interfacial boundary conditions given by Eqs. (79) and (83). This problem is precisely that identified in Eqs. (26)–(29) by homogenizing the variable coefficient two-fluid sharp-interface model via the 'pre-averaging' condition (i.e. Model 4). Similarly, the variable media diffuse-interface model [i.e. Model 1 in Eqs. (30)–(32) or (34)–(36)] reduces to the variable media sharp-interface model [i.e. Model 2 in Eqs. (1)–(3)].

6. Conclusions

Previous homogenization techniques applied to sharp-interface models (AMM) have employed an ad hoc 'pre-averaging' of the interface followed by a more rigorous asymptotic averaging of the governing equations and interfacial conditions [7]. This 'pre-averaging' has been justified previously in AMM by the favorable comparison of the resulting homogenized solution to numerical solutions of slender gravity current problems. In this work, we have examined both sharp-interface and diffuse-interface models of two-fluid flow in heterogeneous porous media in order to understand homogenization theory in the presence of interfaces as well as to provide further justification for the use of the 'pre-averaging' techniques in AMM.

In the analysis of the present paper, the species diffusion in the diffuse-interface models was characterized by a diffusion coefficient D and the length scale of the media variations was characterized by ϵ. We have shown that the limiting case $D \to 0$ (sharp-interface limit) and $\epsilon \to 0$ (leading-order homogenization) can be obtained by two distinct approaches. One approach starts with a variable media, diffuse interface model and first applies a homogenization procedure ($\epsilon \to 0$ with fixed $D > 0$) and then examines the resulting homogenized diffuse-interface model in the sharp-interface limit $D \to 0$. This approach contrasts, but at the same time provides justification for, a second approach which can be viewed as reversing the order in which the above limits are taken. That is, the variable media, diffuse-interface model leads to the variable media, sharp-interface model via a sharp-interface analysis ($D \to 0$ with fixed $\epsilon > 0$). Then, a subsequent homogenization procedure based on methods proposed in AMM lead to a homogenized, sharp-interface model ($\epsilon \to 0$) equivalent to that derived via the first approach. In addition to providing justification for homogenization techniques applied previously to the sharp-interface model directly, analysis of the diffuse-interface model also illuminates the detailed structure of the density field and flow through the interfacial region.

The diffuse-interface model examined here may provide a setting in which other issues involving homogenization of systems involving free surfaces may be carefully investigated. For instance, the homogenization procedures for the sharp-interface models of AMM in non-slender settings, which gave consistent leading-order results, suggested disagreement between the first-order corrections in the bulk

regions and first-order corrections at the interface. An investigation of these corrections in the diffuse-interface model, where interfacial conditions are handled implicitly, may help to resolve such issues. Here the relative scaling of the permeability variations with respect to the diffusive interface length scales may also be important. For example, in the combustion modeling literature it has been documented [16] that predicted behaviors such as front propagation speeds can depend dramatically on the assumptions made regarding how small turbulent lengths scale relative to the interface thickness. It is possible that similar complexities may appear in the present model.

Acknowledgements

The authors would like to acknowledge support from the US National Science Foundation, NSF DMS-0709095 (DMA) and NSF DMS-030868, NSF DMS-0502266 and NSF ATM-0327906 (RMM). The work of CTM was supported by the National Institute of Environmental Health Sciences grant P42 ES05948.

Appendix. One-dimensional solution for $a \to 0$

Here we present a perturbation solution to Eqs. (59) and (60) for $f(s) = 1 + as$. In particular, we let

$$s = s_0 + as_1 + a^2 s_2 + \cdots, \tag{A.1}$$

$$Q = Q_0 + aQ_1 + a^2 Q_2 + \cdots. \tag{A.2}$$

At $O(1)$ we find that

$$\frac{\mathrm{d}^2 s_0}{\mathrm{d}\eta^2} + 2\eta \frac{\mathrm{d}s_0}{\mathrm{d}\eta} = 0, \tag{A.3}$$

$$\frac{\mathrm{d}Q_0}{\mathrm{d}\eta} = 0. \tag{A.4}$$

Taking into account the boundary conditions for Eqs. (59) and (60) we find that

$$s_0 = s^- + \frac{1}{2}(s^+ - s^-)[1 + \mathrm{erf}(\eta)], \tag{A.5}$$

$$Q_0 = 0. \tag{A.6}$$

At $O(a)$ we find that

$$\frac{\mathrm{d}^2 s_1}{\mathrm{d}\eta^2} + 2\eta \frac{\mathrm{d}s_1}{\mathrm{d}\eta} = -\frac{\mathrm{d}}{\mathrm{d}\eta}\left[s_0 \frac{\mathrm{d}s_0}{\mathrm{d}\eta}\right] + (Q_1 - 2\eta s_0)\frac{\mathrm{d}s_0}{\mathrm{d}\eta}, \tag{A.7}$$

$$\frac{\mathrm{d}Q_1}{\mathrm{d}\eta} = 2\eta \frac{\mathrm{d}s_0}{\mathrm{d}\eta}. \tag{A.8}$$

The solution for Q_1 is

$$Q_1 = -\frac{\mathrm{d}s_0}{\mathrm{d}\eta}. \tag{A.9}$$

Then, the equation for s_1 can be reduced to

$$\frac{\mathrm{d}^2 s_1}{\mathrm{d}\eta^2} + 2\eta \frac{\mathrm{d}s_1}{\mathrm{d}\eta} = -2\left(\frac{\mathrm{d}s_0}{\mathrm{d}\eta}\right)^2. \tag{A.10}$$

We can use an integrating factor to integrate this equation once. We obtain

$$\frac{\mathrm{d}s_1}{\mathrm{d}\eta} = -\frac{(s^+ - s^-)^2}{\sqrt{\pi}} \mathrm{e}^{-\eta^2} \mathrm{erf}(\eta) + C\mathrm{e}^{-\eta^2}, \tag{A.11}$$

where C is an arbitrary constant.

At $O(a^2)$ we focus just on the equation for Q_2 which is

$$\frac{\mathrm{d}Q_2}{\mathrm{d}\eta} = -\frac{\mathrm{d}^2 s_1}{\mathrm{d}\eta^2} - 2\left(\frac{\mathrm{d}s_0}{\mathrm{d}\eta}\right)^2 + \frac{\mathrm{d}}{\mathrm{d}\eta}\left(s_0 \frac{\mathrm{d}s_0}{\mathrm{d}\eta}\right), \tag{A.12}$$

so that

$$Q_2 = -\frac{\mathrm{d}s_1}{\mathrm{d}\eta} + s_0 \frac{\mathrm{d}s_0}{\mathrm{d}\eta} - 2\int_{-\infty}^{\eta} \left(\frac{\mathrm{d}s_0}{\mathrm{d}\eta}\right)^2 \mathrm{d}\eta. \tag{A.13}$$

Noting that both $ds_0/d\eta$ and $ds_1/d\eta$ vanish as $\eta \to \infty$ we find that

$$\begin{aligned} Q_2(\eta \to \infty) &= -2\int_{-\infty}^{\infty} \left(\frac{ds_0}{d\eta}\right)^2 d\eta, \\ &= -\frac{2(s^+ - s^-)^2}{\pi} \int_{-\infty}^{\infty} e^{-2\eta^2} d\eta, \\ &= -\sqrt{\frac{2}{\pi}}(s^+ - s^-)^2. \end{aligned} \tag{A.14}$$

Therefore, using the results for Q_0, Q_1 and Q_2 we find that

$$Q(\eta \to \infty) = -\sqrt{\frac{2}{\pi}}(s^+ - s^-)^2 a^2 + \cdots. \tag{A.15}$$

References

[1] C.T. Miller, E.H. Hill III, M. Moutier, Remediation of DNAPL-contaminated subsurface systems using density-motivated mobilization, Environ. Sci. Technol. 34 (4) (2000) 719–724.
[2] E.H. Hill III, M. Moutier, J. Alfaro, C.T. Miller, Remediation of DNAPL pools using dense-brine barrier strategies, Environ. Sci. Technol. 35 (14) (2001) 3031–3039.
[3] D.N. Johnson, J.A. Pedit, C.T. Miller, Efficient, near-complete removal of DNAPL from three-dimensional, heterogeneous porous media using a novel combination of treatment technologies, Environ. Sci. Technol. 38 (19) (2004) 5149–5156.
[4] J.M. Nordbotten, M.A. Celia, S. Bachu, Injection and storage of CO_2 in deep saline aquifers: analytical solution for CO_2 plume evolution during injection, Transp. Porous Media 58 (2005) 339–360.
[5] J.A. Neufeld, H.E. Huppert, Modeling carbon dioxide sequestration in layered strata, J. Fluid Mech. 625 (2009) 353–370.
[6] J.A. Neufeld, D. Vella, H.E. Huppert, The effect of a fissure on storage in a porous medium, J. Fluid Mech. 639 (2009) 239–259.
[7] D.M. Anderson, R.M. McLaughlin, C.T. Miller, The averaging of gravity currents in porous media, Phys. Fluids 15 (2003) 2810–2829.
[8] M.H. Holmes, Introduction to Perturbation Methods, Springer-Verlag, New York, 1995.
[9] E. Weinan, Homogenization of linear and nonlinear transport equations, Comm. Pure Appl. Math 45 (1992) 301–326.
[10] D.M. Anderson, R.M. McLaughlin, C.T. Miller, On gravity currents in heterogeneous porous media, in: Proceedings of the 15th International Conference on Computational Methods in Water Resources (CMWR XV), June 13–17 2004, Chapel Hill, North Carolina, Computational Methods in Water Resources, Volume 1, in: C.T. Miller, M.W. Farthing, W.G. Gray, G.F. Pinder (Eds.), Developments in Water Science, vol. 55, Elsevier Science, Amsterdam, The Netherlands, 2004, pp. 303–312.
[11] O. Tolbert, Numerical inversion of the cell problem for homogenization, Master's Thesis, University of North Carolina at Chapel Hill, 2005.
[12] J.J. Adams, S. Bachu, Equations of state for basin geofluids: algorithm review and intercomparison for brines, Geofluids 2 (4) (2002) 257–271.
[13] D.M. Anderson, G.B. McFadden, A.A. Wheeler, Diffuse-interface methods in fluid mechanics, Ann. Rev. Fluid Mech. 30 (1998) 139–165.
[14] R. Aris, Vectors, Tensors, and the Basic Equations of Fluid Mechanics, Dover, New York, 1962.
[15] D.M. Anderson, G.B. McFadden, A.A. Wheeler, A phase-field model with convection: sharp-interface asymptotics, Physica D 151 (2001) 305–331.
[16] A.J. Majda, P.E. Souganidis, Large scale front dynamics for turbulent reaction–diffusion equations with separated velocity scales, Nonlinearity 7 (1994) 1–30.